The EAS – Top experiment

Campo Imperatore, 2005 m a.s.l.

1985 – 2000

C.Morello

on behalf of the EAS-Top Collaboration

Highlights of Astroparticle Physics - Symposium in memory of Gianni Navarra
Torino, 20 September 2010

ICRC 2005 - A.Watson Rapporteur Paper

γ-ray astronomy : Cygnus X3

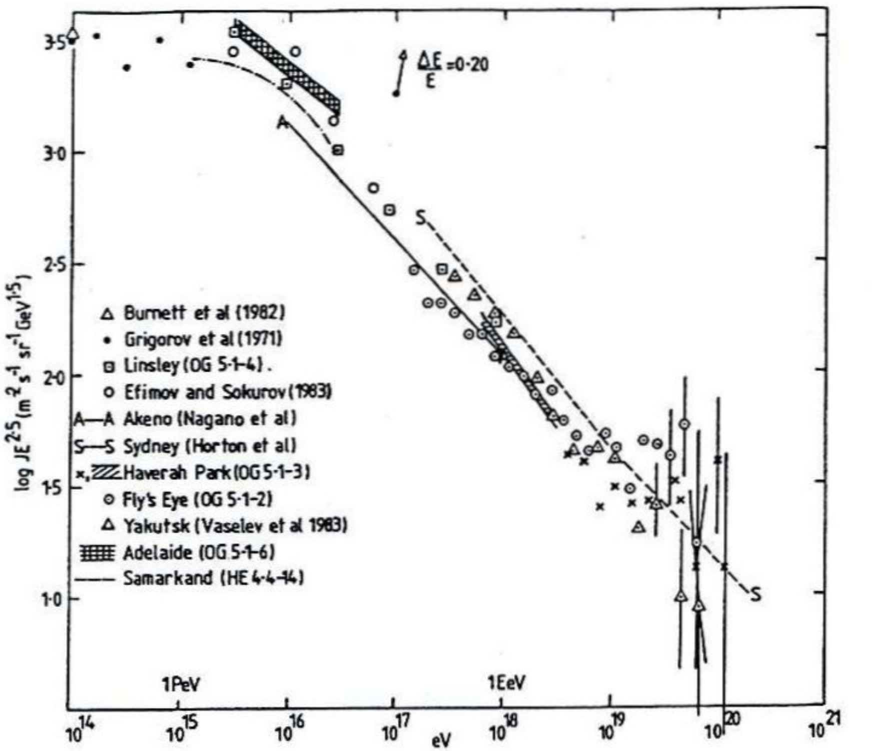

Figure 13:
The differential energy spectrum from 10^{14} – 10^{20} eV. No attempt has been made to normalise data from different experiments. A systematic change in the energy assignment of 20% would shift each point as shown by the arrow; such a systematic effect could well be present in any data set and probably accounts for much of the scatter.

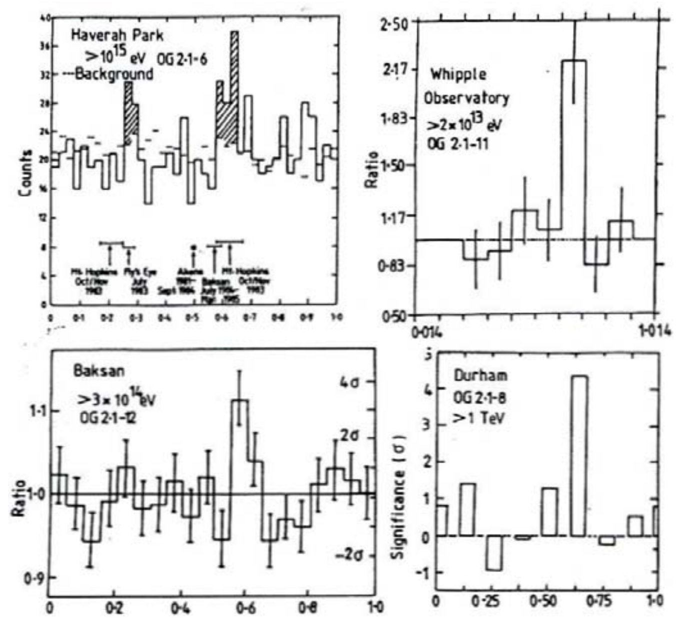

Figure 1: Cygnus X-3 light curves as determined from recent observations at different energies.

Fluxes near the sensitivity of the arrays

Abnormal muon content of showers from Cygnus X3 ?

Needs: improved sensitivity, connection with direct measurements, knowledge of the total primary energy and detailed study of the shower characteristics ➔ detection of different EAS components + connection with underground muon detectors (average depth ~ 3100 m water eq.) ➔ site location and primary energy range

EAS-TOP at LNGS

Campo Imperatore
2000 m a.s.l.   820 g·cm^{-2}
data taking: 1989-2000
$10^{13} \leq E_0 \leq 10^{16}$ eV

The EAS-TOP multi-component detector

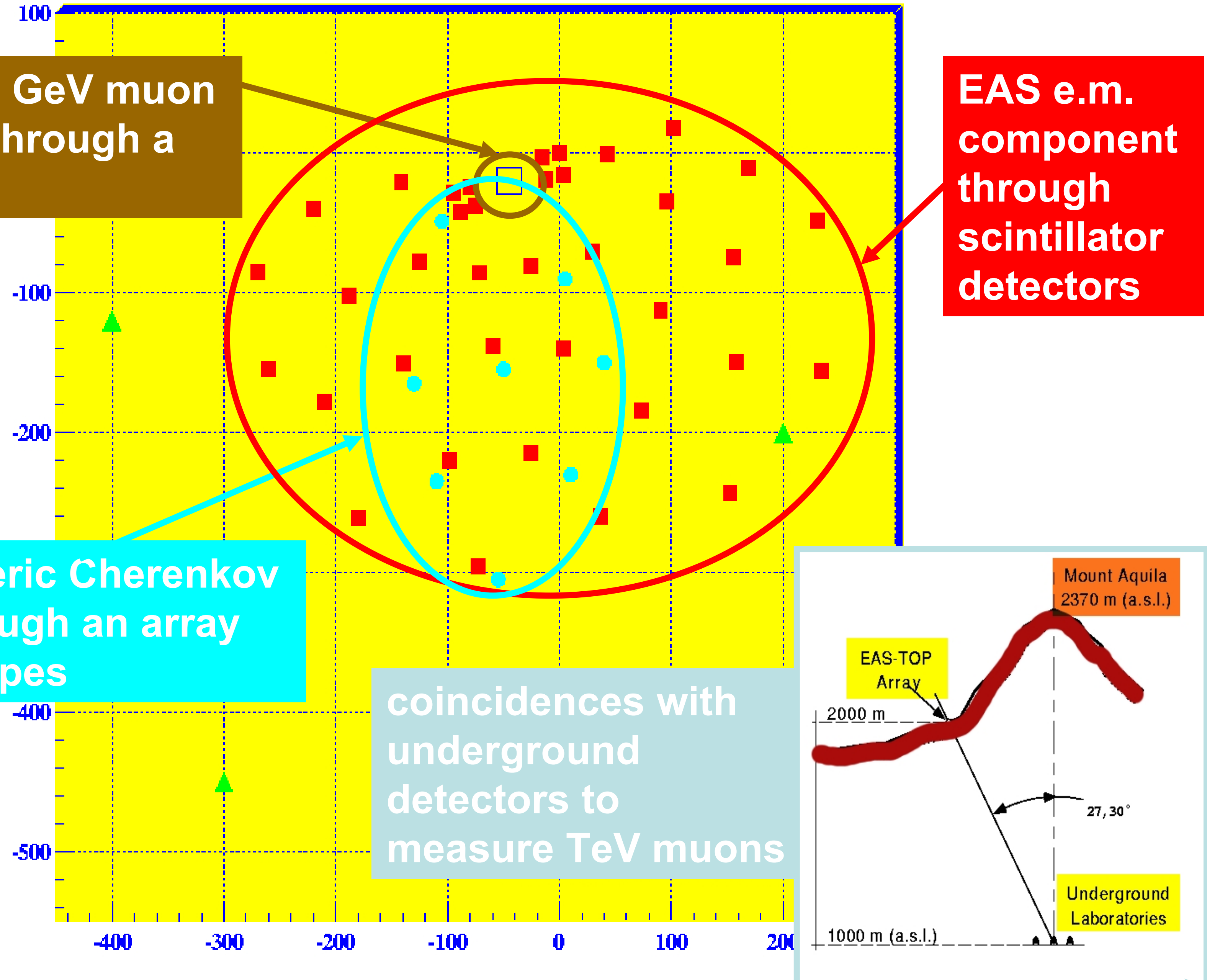

hadrons and GeV muon component through a calorimeter

EAS e.m. component through scintillator detectors

Atmospheric Cherenkov light through an array of telescopes

coincidences with underground detectors to measure TeV muons

N.I.M A277 (1989) 23

The e.m. detector

37 scintillation modules, 10 m^2 each; total area 10^5 m^2. Each module split into 16 individual scintillators, 2 PMTs each for arrival direction and density particle measurements up to 400 particles m^{-2}

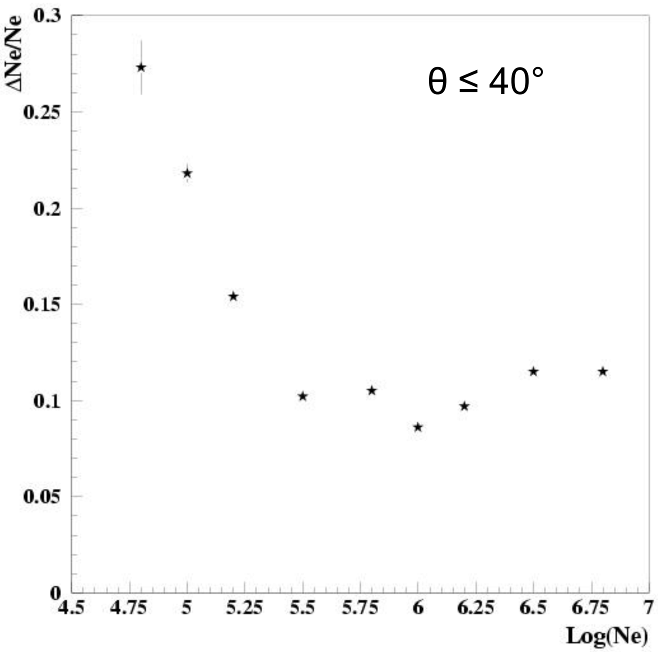

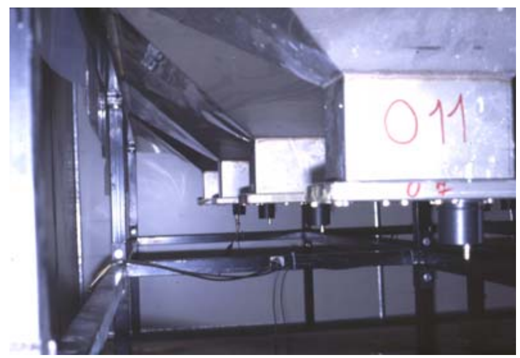

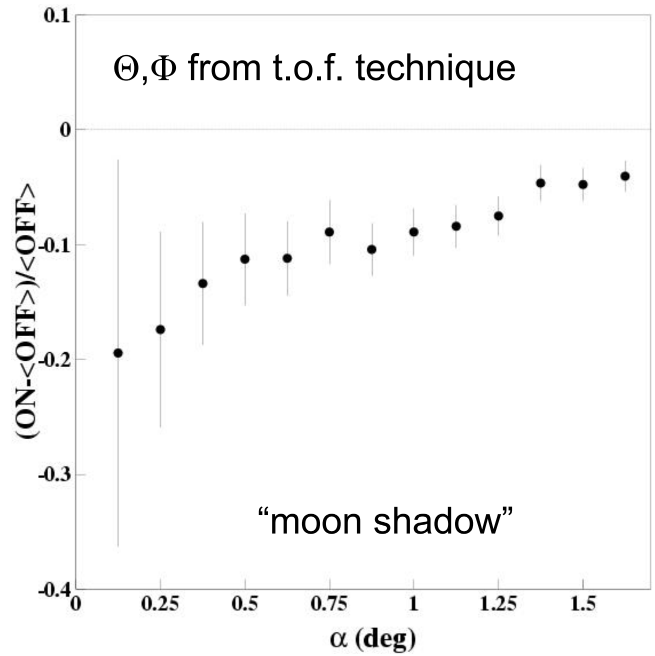

N_e, X_{core}, Y_{core}, s (slope of the l.d.f. with the NKG formalism) reconstructed from particle density measurements.

Resolutions: $\sigma_{Ne}/Ne \approx 0.1$ $\sigma_{\Delta Xcore} = \sigma_{\Delta Ycore} \approx 5$ m $\sigma_s \approx 0.1$

Arrival direction: $\sigma_\vartheta \approx 0{,}83°$ all internal events $\approx 0.5°$ internal events $Ne > 10^5$

N.I.M. A 420 (1999) 117

The muon – hadron detector (MHD)

144 m^2 calorimeter
12x12x3 m^3

Each layer:
13 cm Fe absorber,
2 layers streamer tubes + 1 operating in "quasi-proportional" mode.

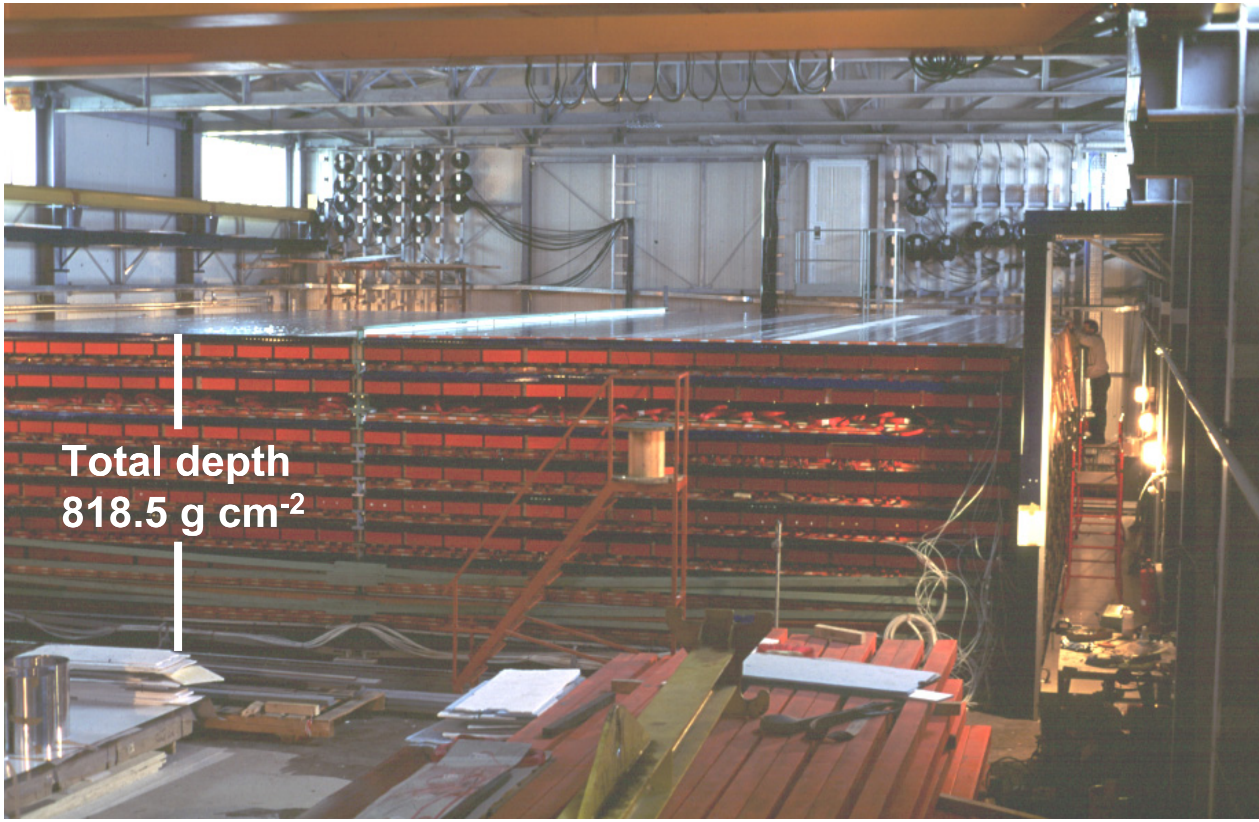

Streamer tubes (100 μm wire, HV=4650 V, 368 in each layer). Bi-dimensional readout (anode wires + orthogonal Y strips).
Used as μ tracking device (E_μ>1 GeV).

QP tubes (50 μm wire, HV=2900 V) operate in saturated proportional mode. Signal charge collected by 840 pads (40x38 cm^2).
Used for hadron calorimetry (E_h>30 GeV) and EAS core study.

Astrop. Physics 6 (1997) 43

The Cerenkov detector

8 telescopes: 2 wide angle detectors f.o.v. 0.16 sr, 1 mpx PMT each

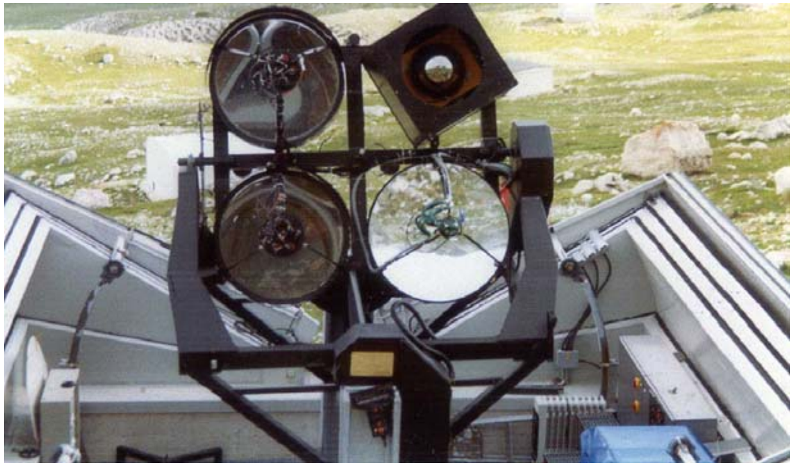

mpx PMT (96 pixels) for Cerenkov light observations (E_0 > 10 TeV)

“Wide angle camera” (E_0 > 40 TeV) for correlated observations with MACRO and LVD experiments

Cosmic Ray physics with EAS-TOP

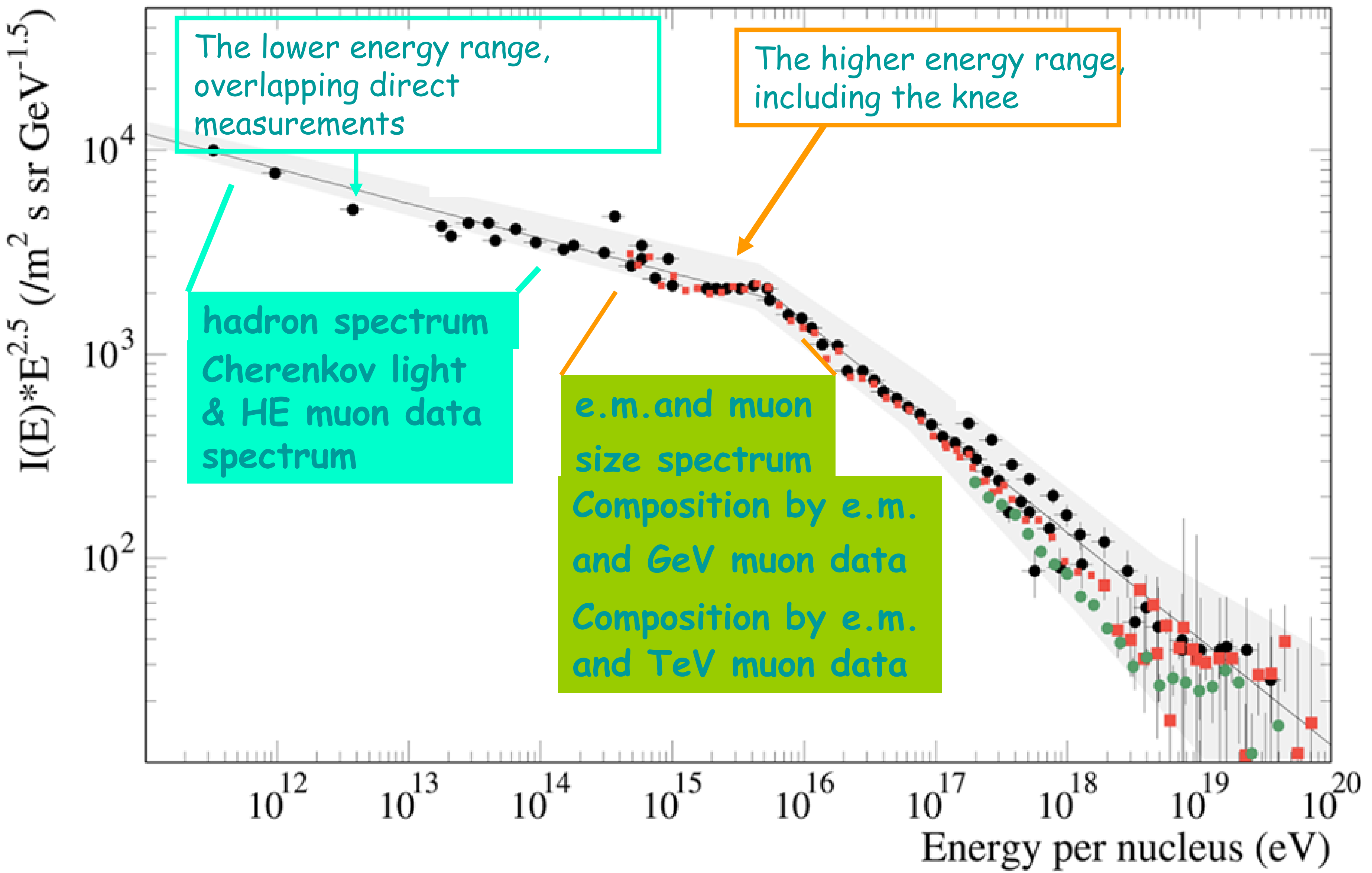

DETECTORS & METHODS

Hadrons ➔ p-spectrum @ E_0 ~ 0.5 - 50 TeV

Cherenkov light + TeV muons ➔ p, He, CNO fluxes @ E_0 ~ 100 TeV

e.m. ➔ spectrum in “knee” region E_0 ~ 10^3 - 10^4 TeV

e.m. + GeV muons ➔ composition in “knee” region

e.m. + TeV muons ➔ composition in “knee” region

e.m. ➔ anisotropies & search for gamma primaries

Verifications of methods and HE physics used

➔ CORSIKA-QGSJET ⇐

Astrop. Phys. 19 (2003) 329

Hadron Measurements

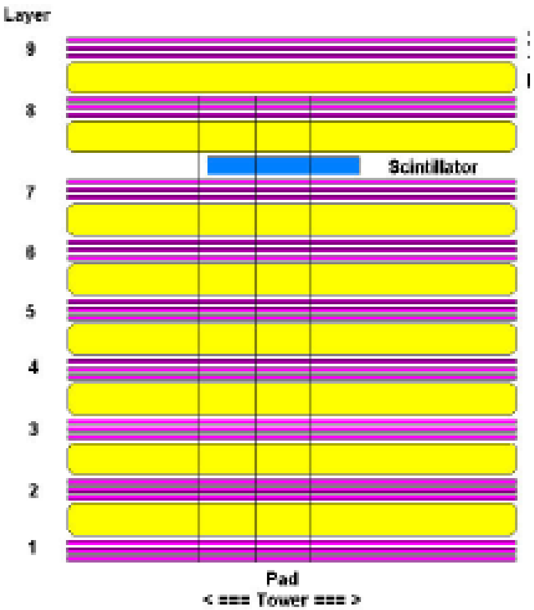

Local hadron trigger ≥30 m.i.p. (30 GeV)

Pattern recognition: clusters in each layer, position weighted by charge.

Hadron: ≥ 3 consecutive planes (7th included), E_{max} on the central pad

Test at CERN-PS e^+ beam:
hadrons up to 650 GeV

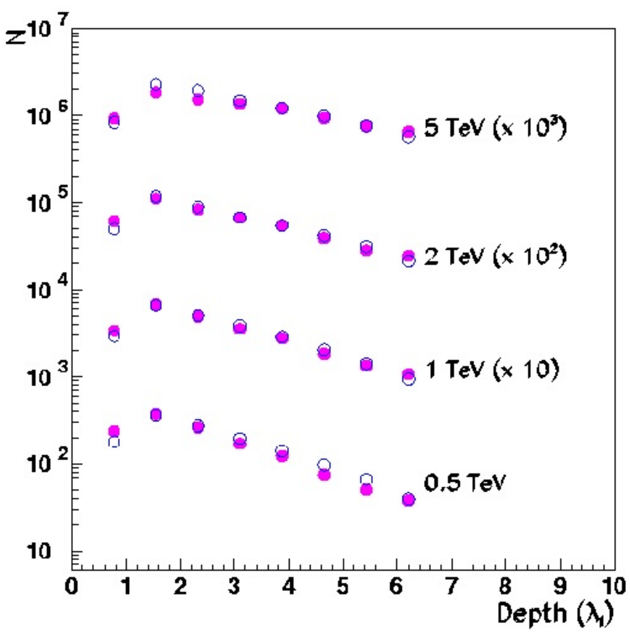

Above 1 TeV:
comparison of simulated and measured transition curves for hadronic showers

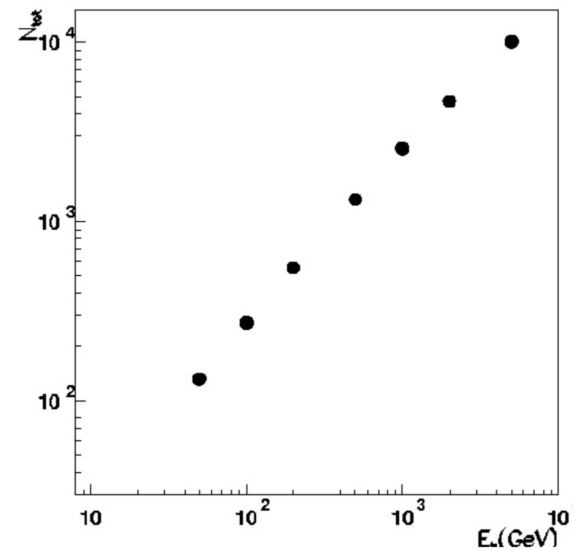

Astrop. Phys. 19 (2003) 329

Hadron Measurements

From 10^6 events in 615 days : 40832 survived the trigger

$$N_{exp}(E_h - E_h + dE_h, x) = \int_{\Omega}\int_{\Delta E_h} S(E_h,\Theta,x)\, T\, A(E_h,\Theta)\, d\Omega\, dE_h$$

$$S_{had}(E) = (2.25 \pm 0.21 \pm 0.34^{sys}) \times 10^{-7} (E_h/1000)^{(-2.79 \pm 0.05)} \ (m^2 s\ sr\ GeV)^{-1}$$

Statistical error +
14% energy dependent systematic uncertainty (detector acceptance, energy determination, technical calibration, angular distribution of hadrons in the simulation)

15% Systematic uncertainty due to the different scintillators

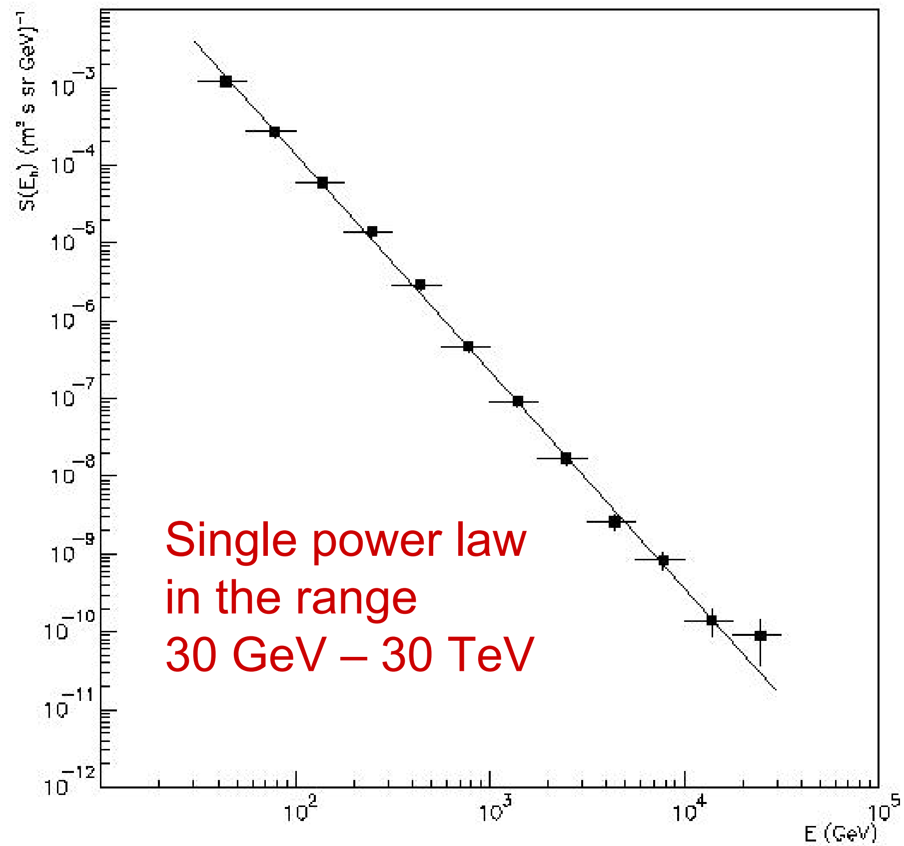

Astrop. Phys. 19 (2003) 329

Hadron Measurements

The primary proton spectrum is derived: a) checking the hadron propagation code in atmosphere; b) subtracting from hadron spectrum the contribution of He primaries (15% RUNJOB, 29% JACEE @ 1 TeV; <10% heavier nuclei); c) $\chi 2$ minimization of the difference between MC and experimental hadron fluxes)

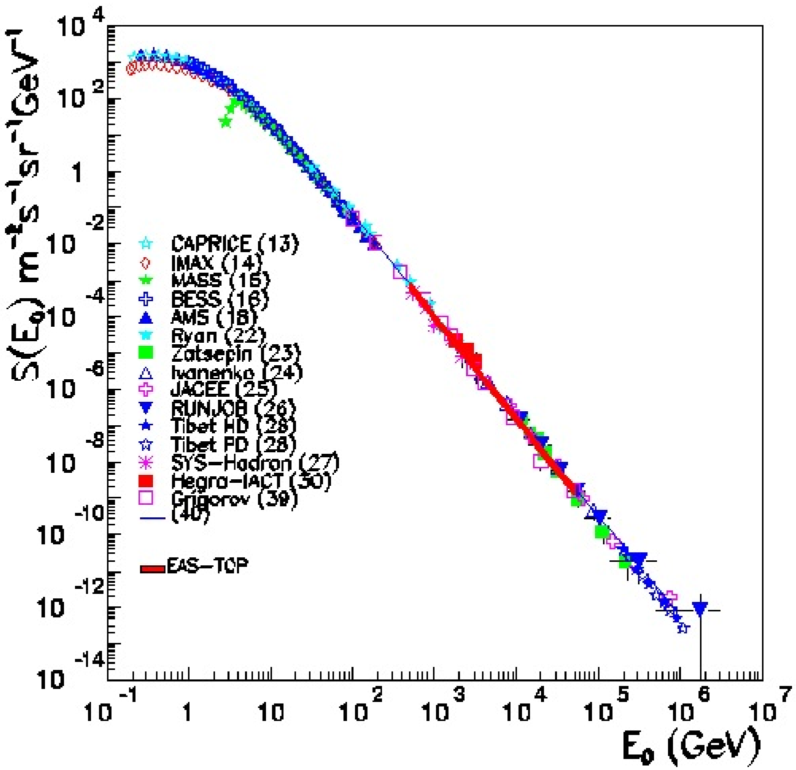

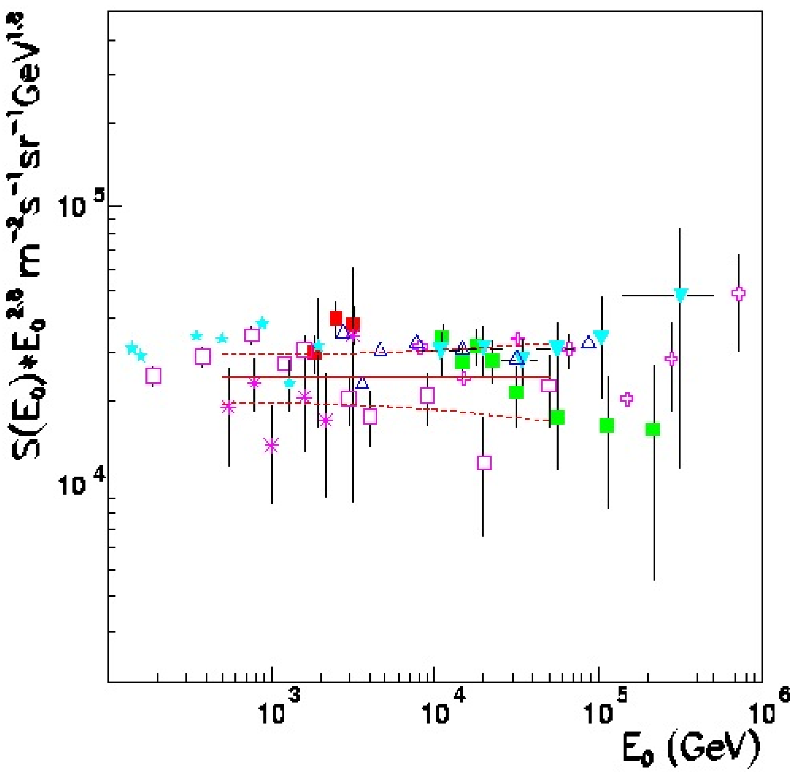

$S(E) = (9.8 \pm 1.1 \pm 1.6\text{sys}) \times 10^{-5} (E/1000)^{(-2.80 \pm 0.06)} (m^2\ s\ sr\ GeV)^{-1}$

Compatible with a single power slope in ΔE = 0.5 – 50 TeV

p, He and CNO fluxes @ 100 TeV from MACRO and EAS-TOP

(separation 1100-1300 m of rock: $E_\mu \approx 1.3 - 1.6$ TeV)

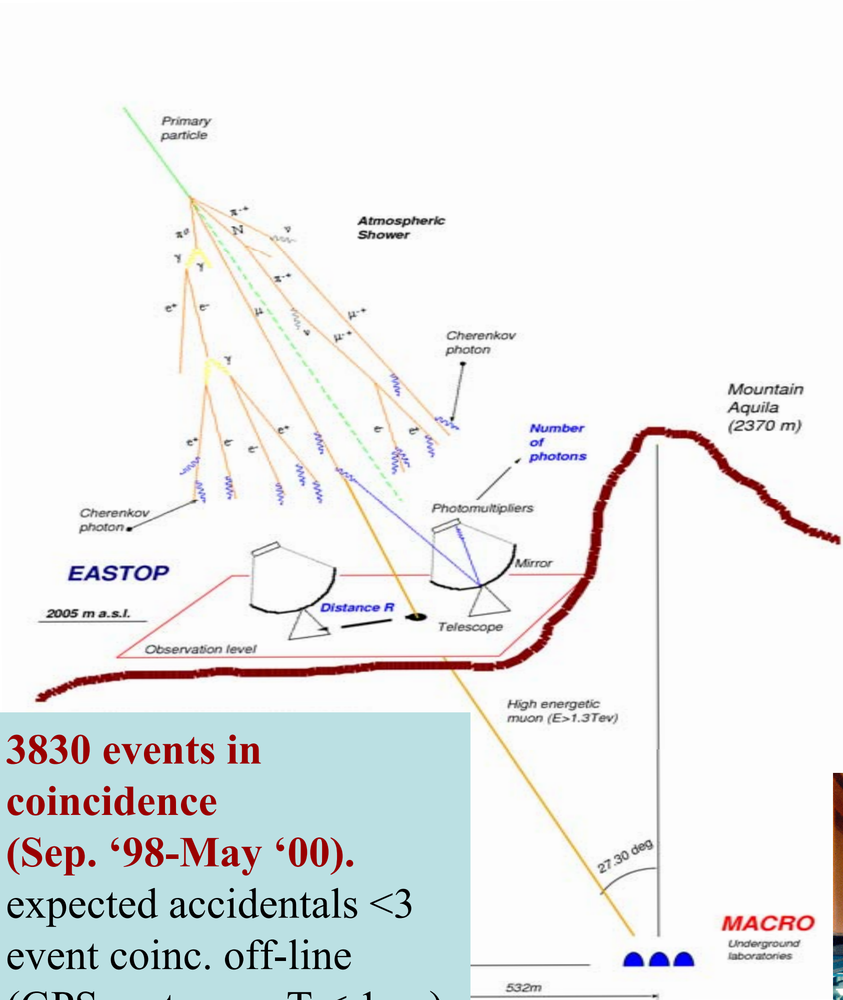

3830 events in coincidence (Sep. '98-May '00).

expected accidentals <3

event coinc. off-line

(GPS system - σT < 1ms)

EAS-TOP (Cherenkov detector): total energy through the detected atmospheric Cherenkov light signal.

E_{th} > 40 TeV

MACRO (muon detector): EAS primaries with E_μ > 1.3 TeV/n; EAS geometry through the μ tracks.

(r ~ 20 m, θ ~ 1^0 uncertainties)

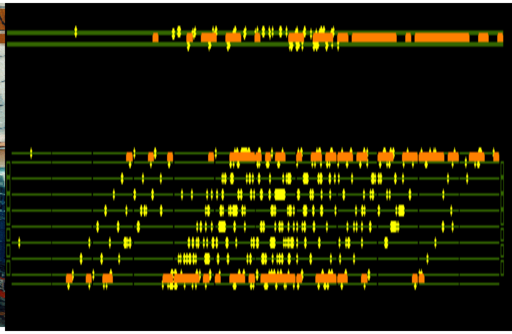

Astrop. Phys. 21 (2004) 223

Astrop. Phys. 21 (2004) 223

C.I. + TeV muon analysis

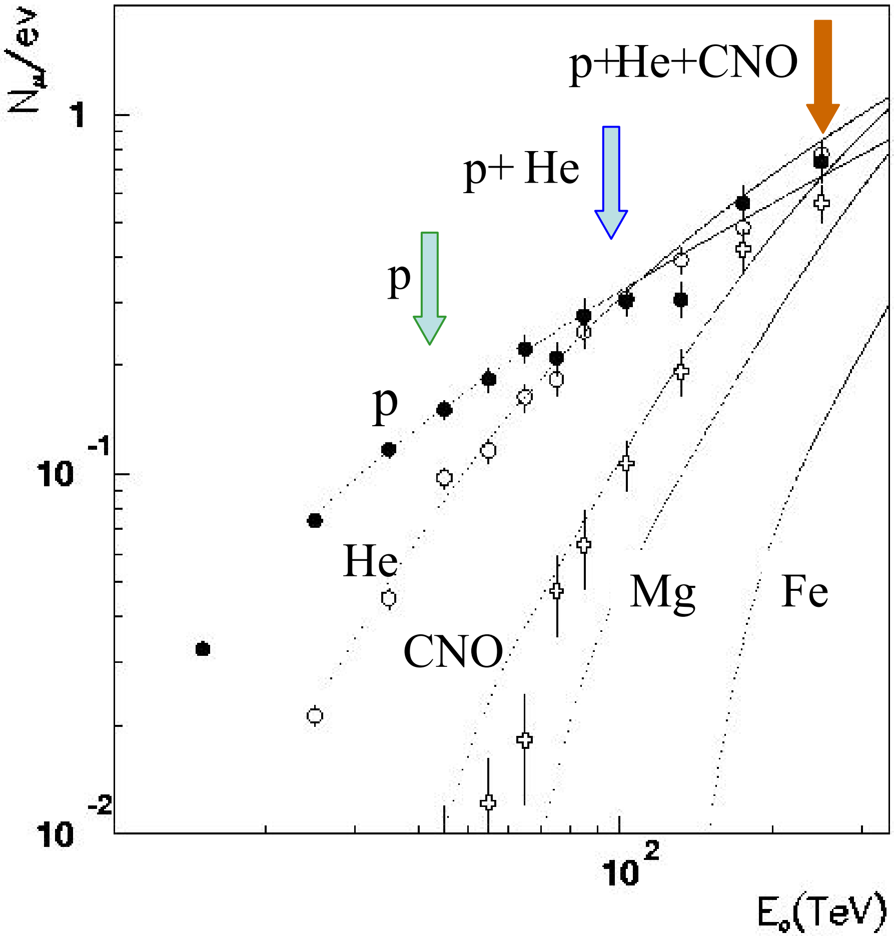

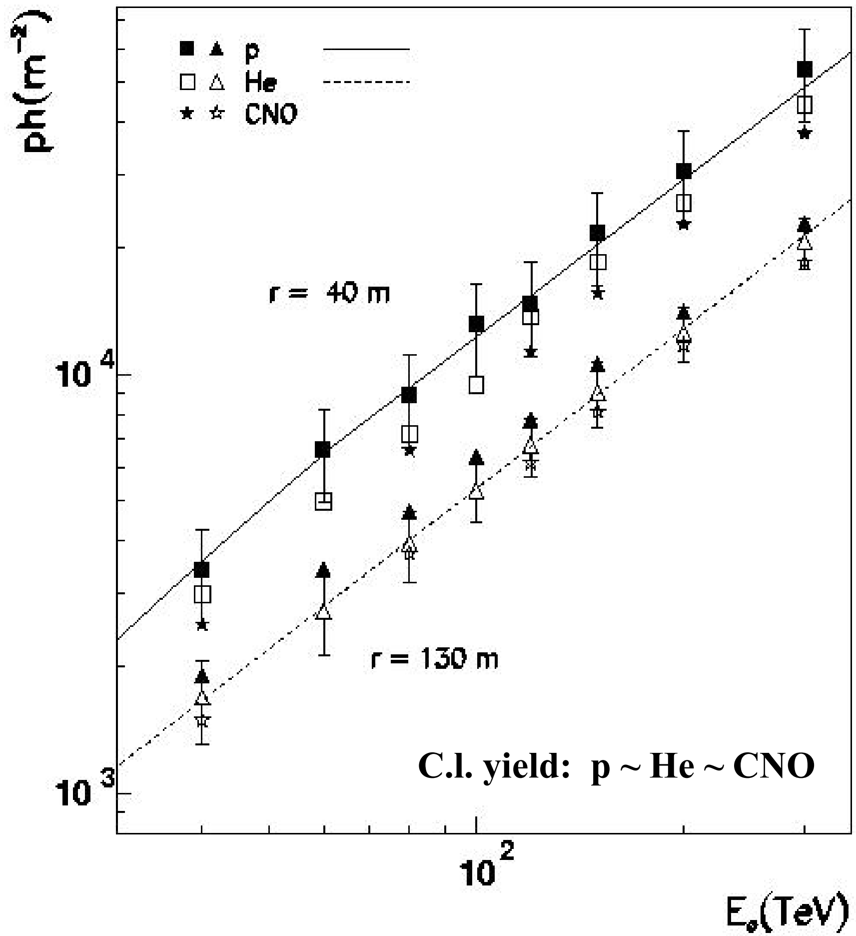

Beams are well defined:

- p at E_o < 40 TeV
- p+He at 40 < E_o < 100 TeV
- p+He+CNO at E_o > 100 TeV

E ≈ 80 TeV $N_\mu^p \approx N_\mu^{He}$

E ≈ 250 Tev $N_\mu^p \approx N_\mu^{He} \approx N_\mu^{CNO}$

Same efficiency (inside 15%) in TeV μ production.

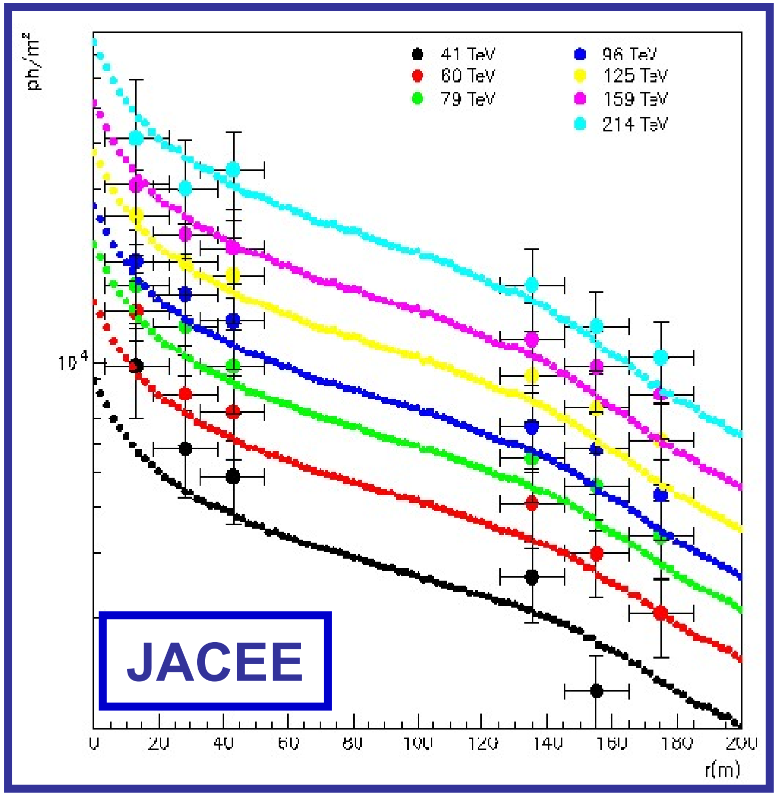

Simulated and real photon densities vs core distance. Simulated lateral distributions obtained by weighting together p,He and CNO lateral distributions according to JACEE and RUNJOB spectra.

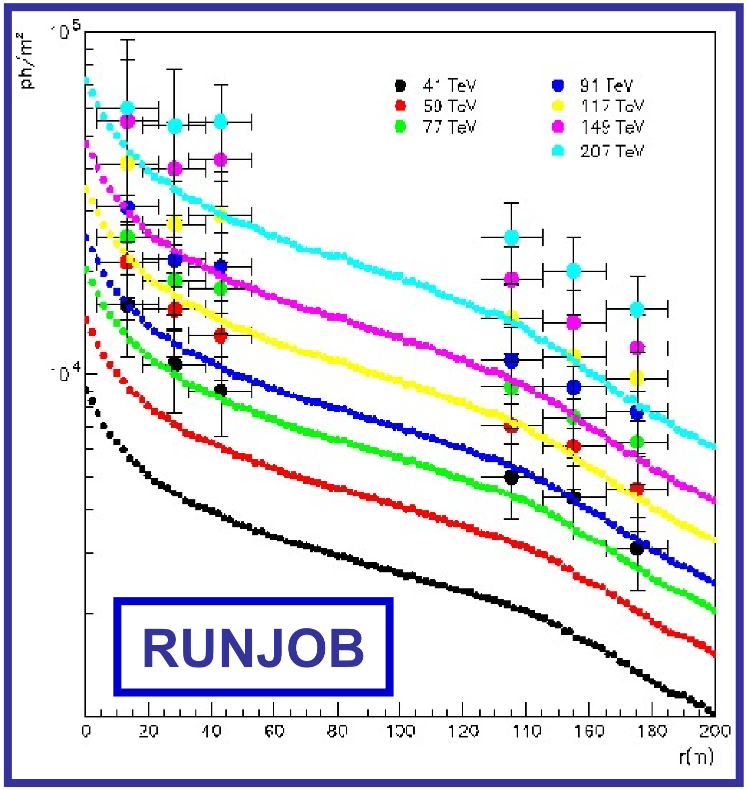

Data are in good agreement (within 20% systematic uncertainties)

A harder He spectrum like JACEE fits better the data

p, He, CNO @ ~ 100-200 TeV

p+He p+He+CNO

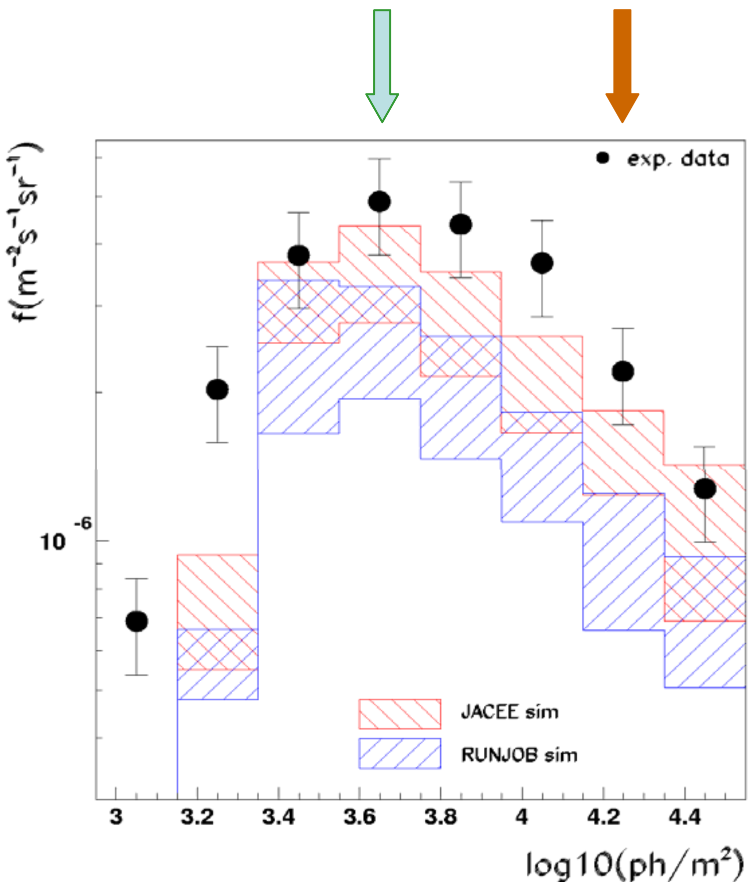

Information	EAS-TOP & MACRO	JACEE	RUNJOB
J_{p+He} (80 TeV)	18 ± 4	12 ± 3	8 ± 2
$J_{p+He+CNO}$ (250 TeV)	1.1 ± 0.3	0.7 ± 0.2	0.5 ± 0.1
J_p / J_{p+He} (80 TeV)	0.29 ± 0.09	0.45 ± 0.12	0.63 ± 0.20
$J_{p+He} / J_{p+He+CNO}$ (250 TeV)	0.78 ± 0.17	0.70 ± 0.20	0.76 ± 0.25
J_{He} (80 TeV)	12.7 ± 4.4	6.4 ± 1.4	3.1 ± 0.7

x 10^{-7} $m^{-2}s^{-1}sr^{-1}TeV^{-1}$

EAS-TOP & MACRO data

EAS-TOP & MACRO data + p-flux

Astrop. Phys. 21 (2004) 223

Astrop. Phys. 10 (1999) 1

Electromagnetic Size spectrum

Ne

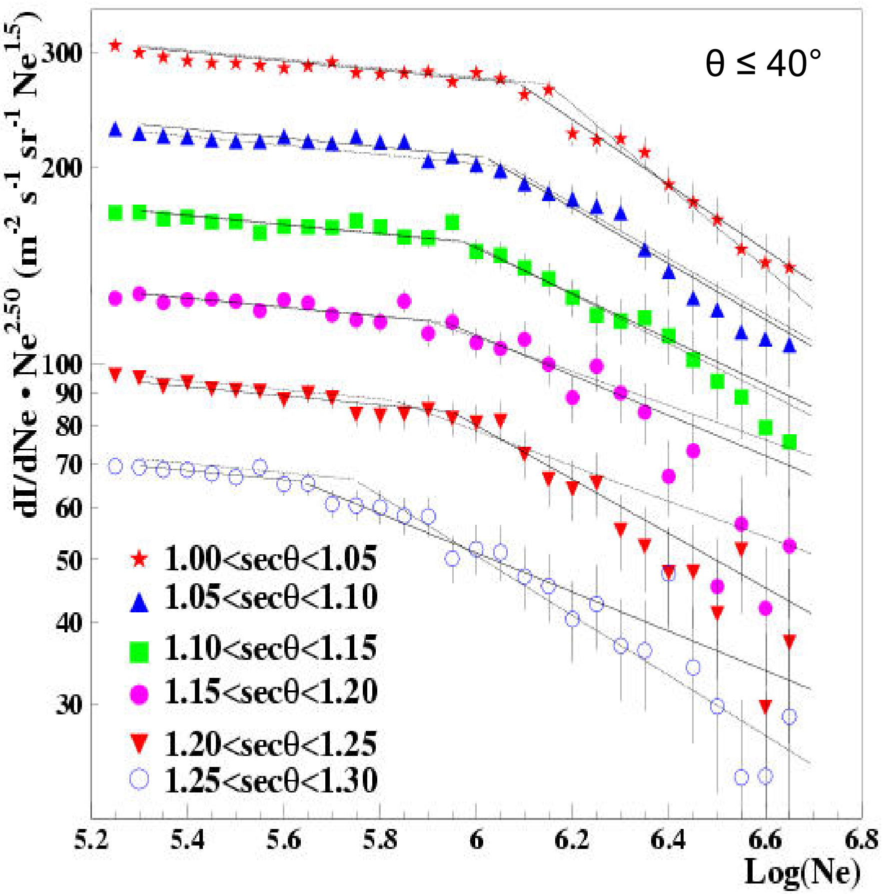

Λ_{EAS} = (219 $\pm$ 3) g cm^{-2}

Λ_{knee}= (222 $\pm$ 3) g cm^{-2}

"Normal behaviour" of showers concerning the absorption in atmosphere and the integral intensity at different atmospheric depth => effect occurring at given primary energy.

Change of slope seen at all zenith angles. Shifts as expected with atmospheric depth.

Below the knee the size spectrum agrees with extrapolation of direct measurements.

The break is sharp. It can be represented by two power law intersecting spectra.

The shower size at the knee attenuates with increasing atmospheric depth; its attenuation lenght is compatible with the attenuation of EAS particles in the same energy range.

Astrop. Phys. 10 (1999) 1

All particle energy spectrum

Conversion from primary energy and mass to EAS size by means of complete simulations of the cascades in atmosphere: Corsika – HDPM code

$$N_e(E_o, A) = \alpha(A)\, E_o^{\beta(A)}$$

Effective A from extrapolation of single nuclear spectra from direct measurements

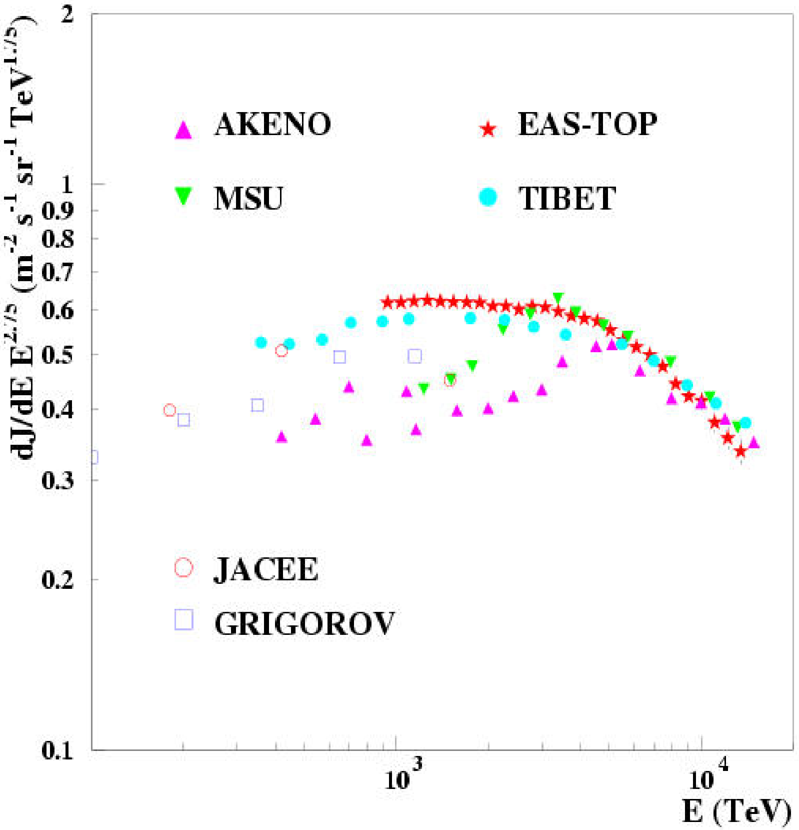

$\Theta < 40°$ 810 gr cm^{-2}

Knee @ 3.4 x 10^{15} eV for Helium

Below the knee: γ = 2,76 ± 0,03

(900 TeV – 2300 TeV)

Above the knee γ = 3.19 ± 0,06

(5000 TeV – 4000 TeV)

Sistematic uncertainties ± 10 %

Below the knee well connected with ballon/satellites experiments; above the knee good agreement with existing EAS data.

Astrop. Phys. 21 (2004) 583

e.m. and GeV muon size spectra

Ne

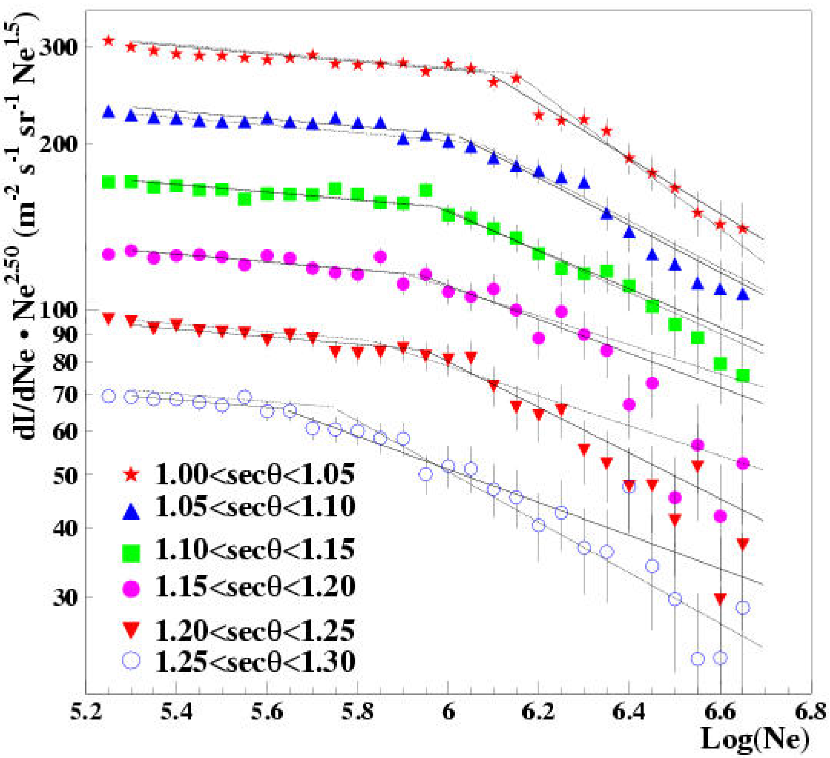

Nμ

MHD: > 6 hit tubes in 3 layers
180<r<210m, Nμ180 , ρ_μ180

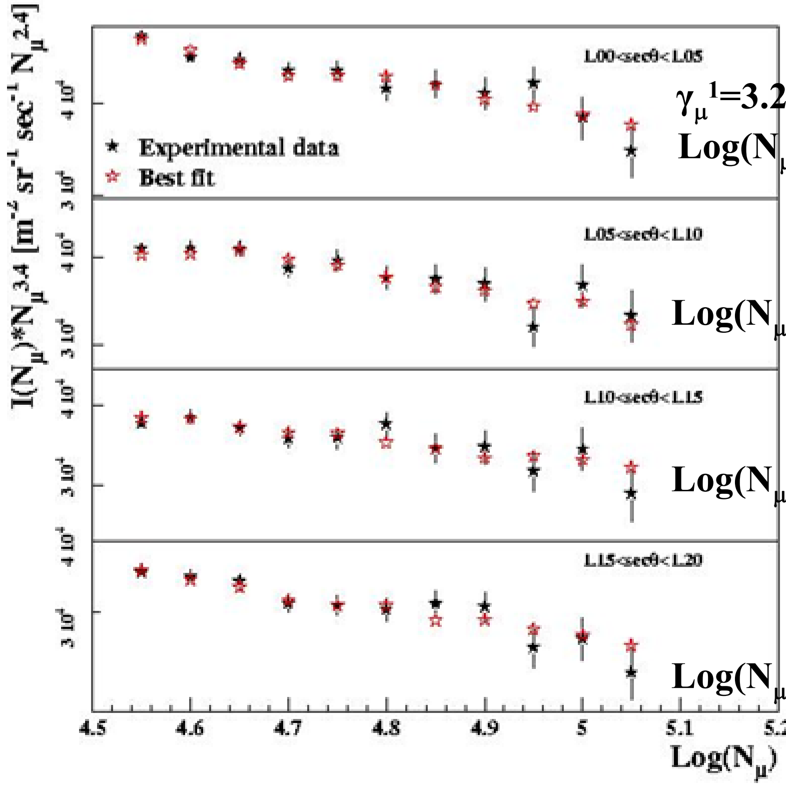

$$\frac{dI}{dN_{e,\mu}} = S_{ke,\mu}\left(\frac{N_{e,\mu}}{N_{ke,\mu}}\right)^{-\gamma^{1,2}_{e,\mu}}$$

2 slopes fits to the N_e and N_μ spectra

Integral fluxes around the knee consistent inside the experimental errors.

Change in slope of N_μ spectra not self evident as the whole shape is affected by poissonian fluctuations.

Astrop. Phys. 21 (2004) 583

Composition from e.m. and GeV muon data

Consistency of the Ne, Nμ spectral slopes and of the intensities at the break: are we observing the spectra of the same dominating component ?

Experimental spectra compared with the simulated ones for single components (p, He, CNO, Fe).

For each component: primary energy spectrum fitting the experimental e.m. size spectrum.

From such energy spectrum the muon size flux is obtained and compared to the experimental one.

Astrop. Phys. 21 (2004) 583

Composition from e.m. and GeV muon data

Measured and expected muon intensities for different primaries on the base of the Ne spectrum

If "Knee" on Helium primaries

$E_{k(He)}$ = (3.5 ± 0.3) 10^{15} eV

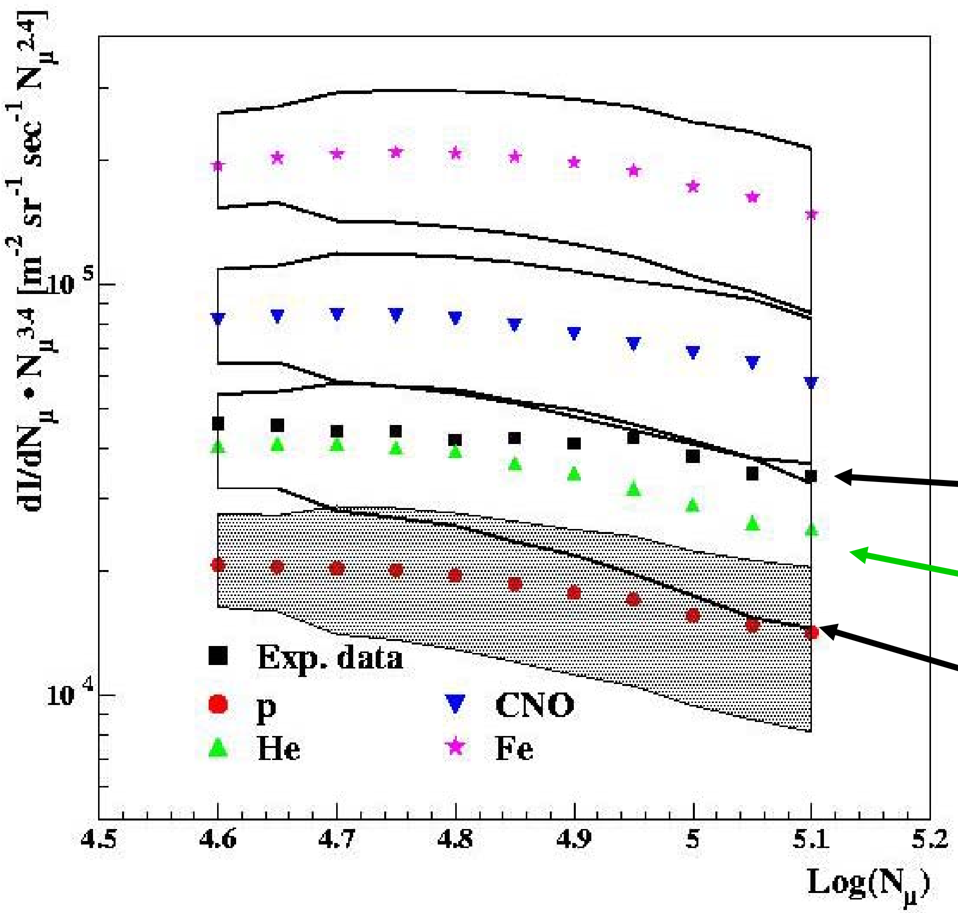

Upper and lower limits derived from differencies between extreme predictions of different interaction models

VENUS

QGSJET

NEXUS

Simulated proton and CNO spectra hardly compatible with experimental data. Best agreement with Helium;

Astrop. Phys. 21 (2004) 583

Evolution of the primary composition

CORSIKA/QGSJET + GEANT
Primary spectra with g=2.75
p, He, N, Mg, Fe

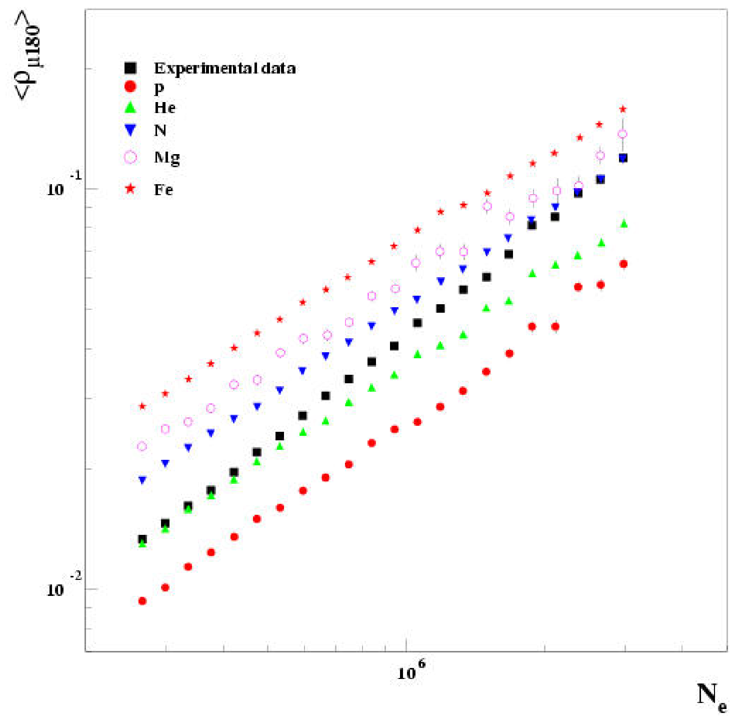

Good agreement at the lower energies with direct measurements

Muon density increasing with shower size from He to CNO.

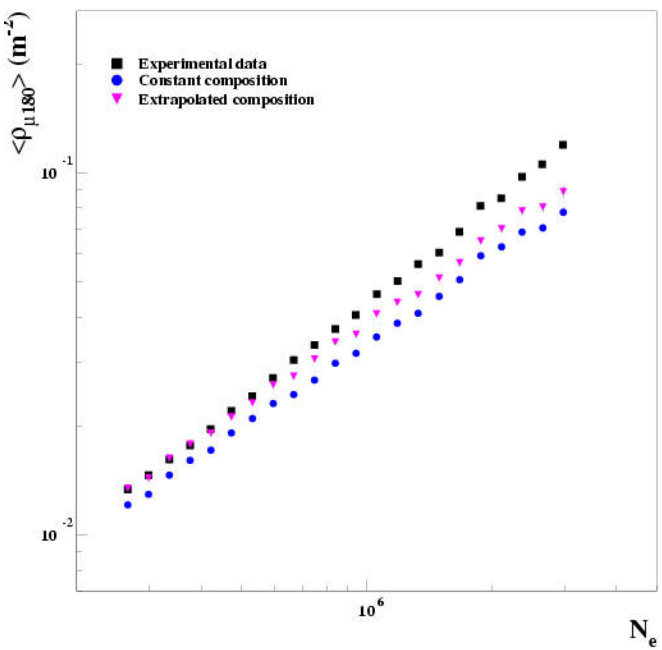

Experimental muon density compared with simulations based on:

- constant primary mass composition from direct measurements at 1 TeV.
- Extrapolated primary composition from direct measurements with different slopes for protons and heavier components as suggested by JACEE: no change of spectral indexes at the knee.

Astrop. Phys. 21 (2004) 583

Evolution of abundances

Fit of the experimental $N_{\mu 180}$ distributions with different compositions.
Good description of data with a 3-component composition: light (p+He) + intermediate (N) + heavy (Fe)

Below the knee

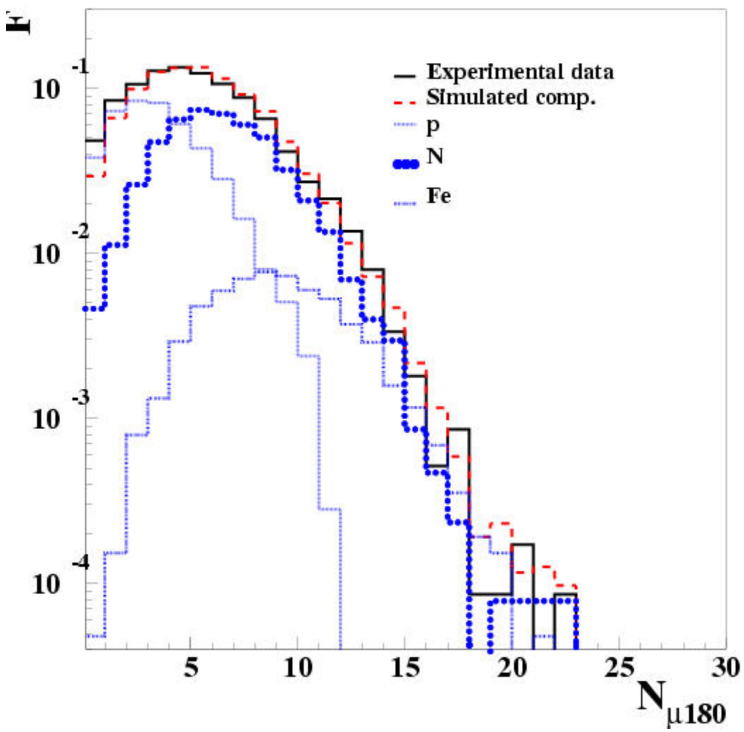

Above the knee

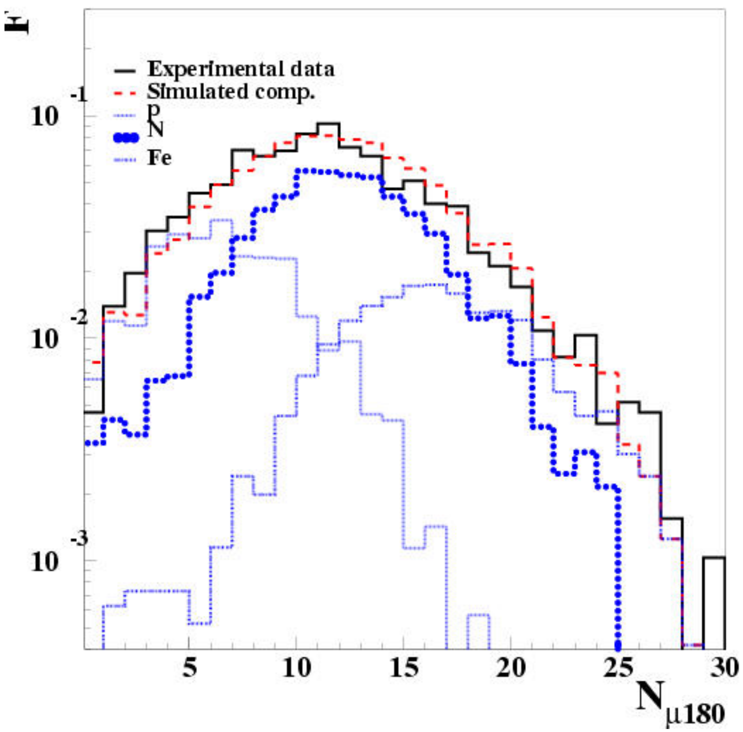

Decreasing weight of the light component

Astrop. Phys. 21 (2004) 583

The composition in the ‘knee’ region

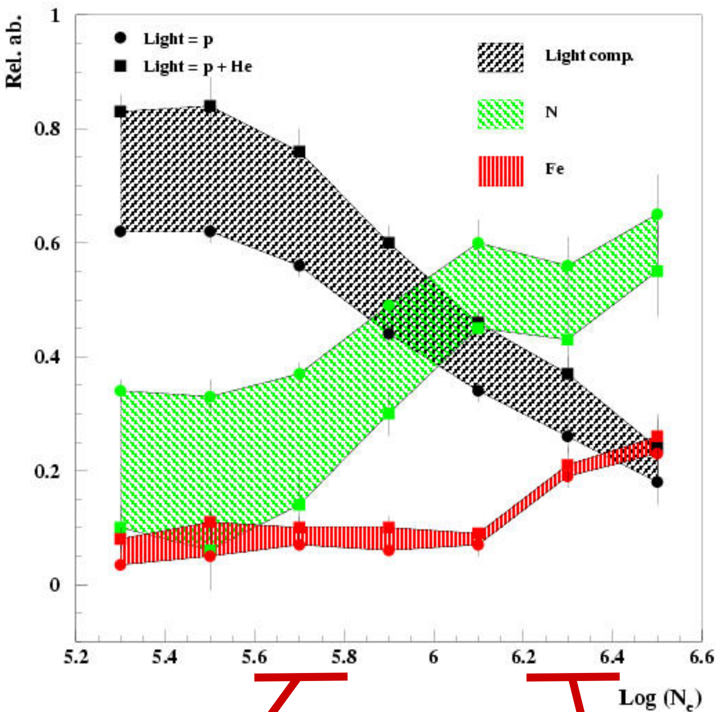

0.76 (p+He)
0.14 (N)
0.10 (Fe)

0.37 (p+He)
0.43 (N)
0.21 (Fe)

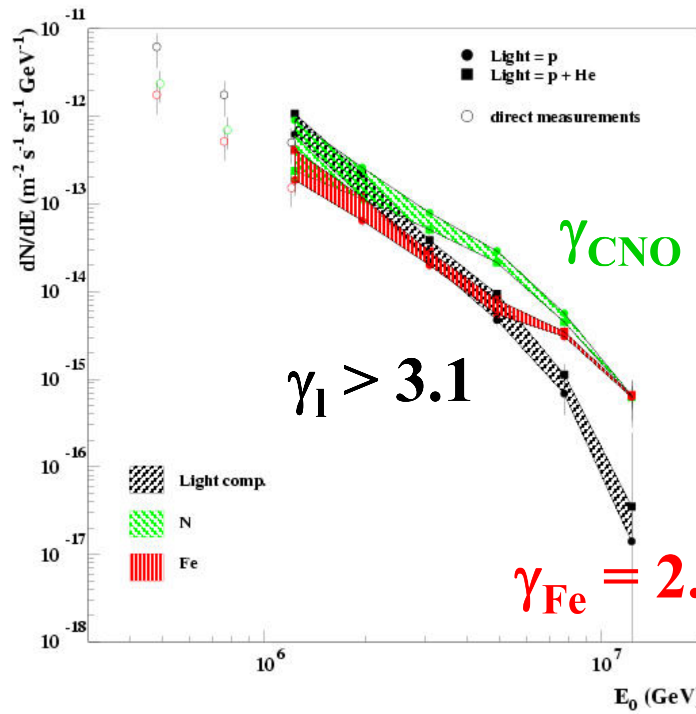

$\gamma_{CNO} \sim 2.75$

$\gamma_l > 3.1$

$\gamma_{Fe} = 2.3 – 2.7$

Heavier primary have harder spectra ➔ $E_k \propto Z$?

Astrop. Phys. 20 (2004) 641

10^{15} – 10^{16} eV: composition from e.m. and TeV muon data

Study of TeV muon multiplicity distribution in selected intervals of N_e around the knee: size Ne from EAS-Top and HE muons Nm (Eμ > 1.3 TeV) from MACRO

HE Muons are produced in the early stages of development: they come from a kinematic region beyond the central rapidity region.
Test of consistency of the model in a wide range of rapidity region

Simulation with
CORSIKA/QGSJET
10^2-10^5 TeV
5 mass groups

Resolutions allow a maximum of 2 component separation inside the primary beam

L = p + He

H = Mg + Fe

L+H

Measured

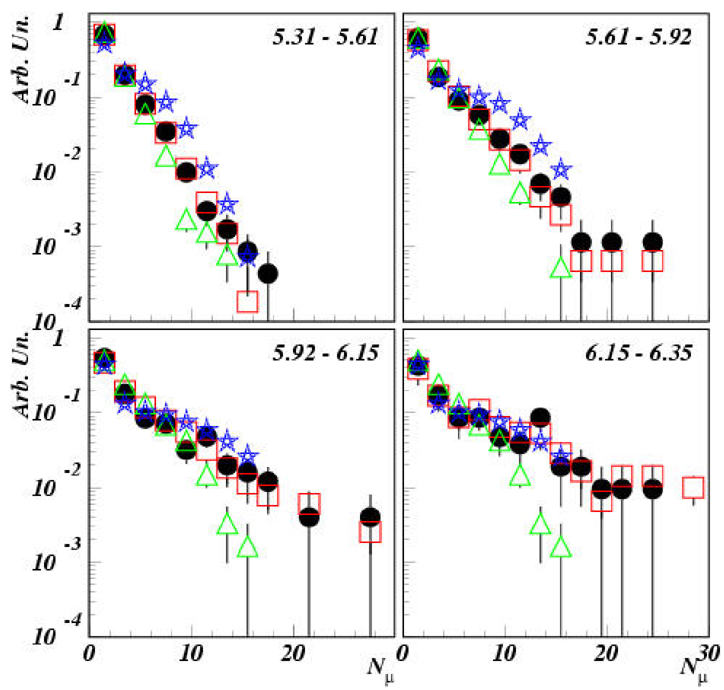

Uncertainties in the TeV muon production due to the choice of model are <10% (E_0>100 TeV/n)

Astrop. Phys. 20 (2004) 641

For each N_e window:

$$\chi^2=\Sigma_i \frac{(N_i^{exp} - p_L N_i^L - p_H N_i^H)^2}{(\sigma_i^{exp})^2+(p_L\sigma_{iL})^2 + (p_H\sigma_{iH})^2}$$

Spectrum across the knee

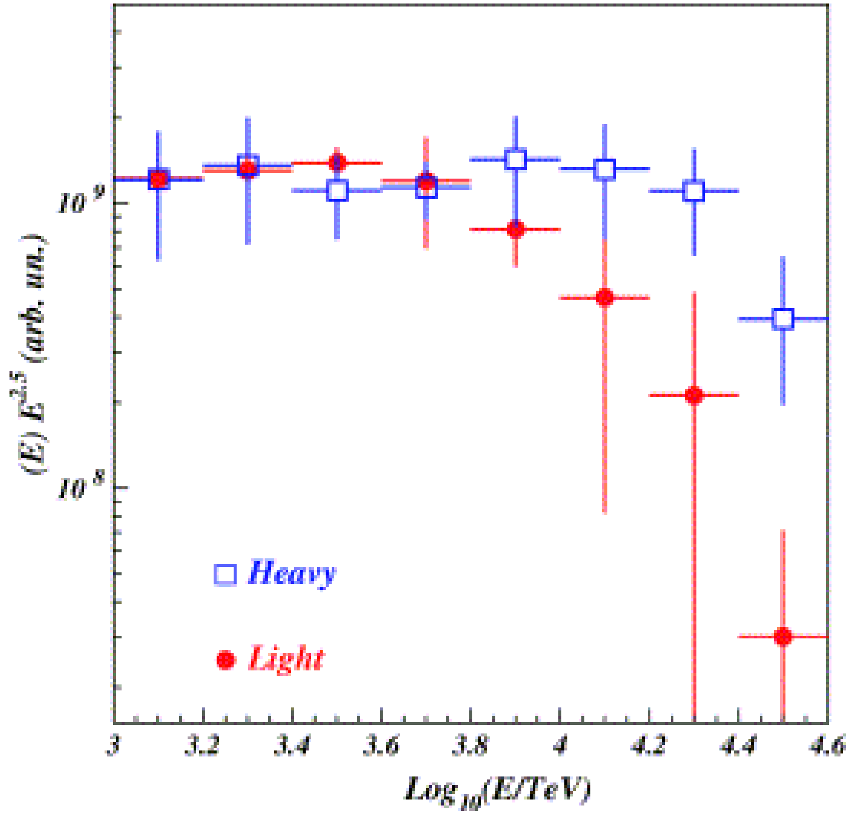

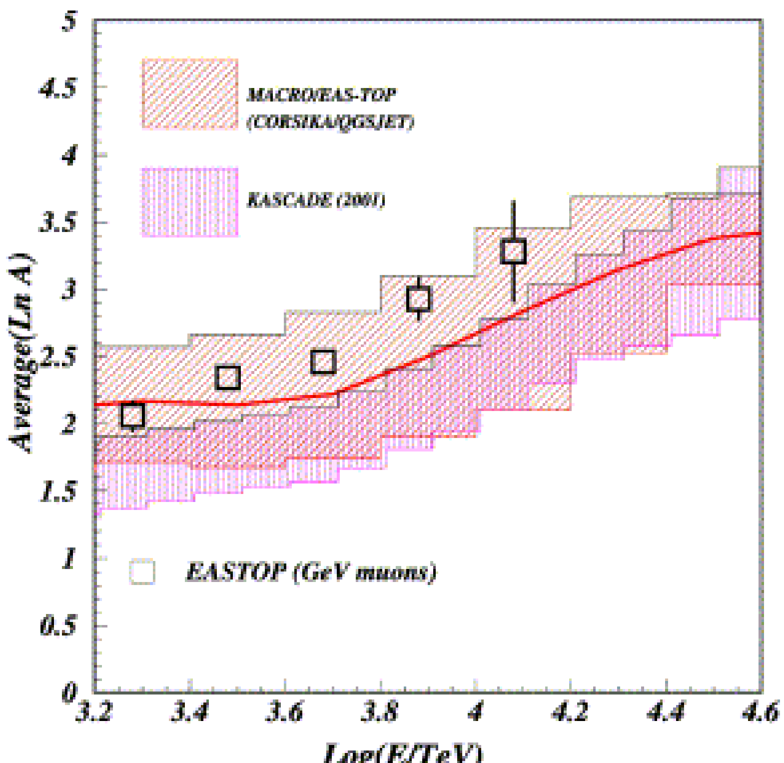

Increase in <logA> across the knee

consistency of the model among GeV and TeV muons

The primary spectrum from EAS-TOP

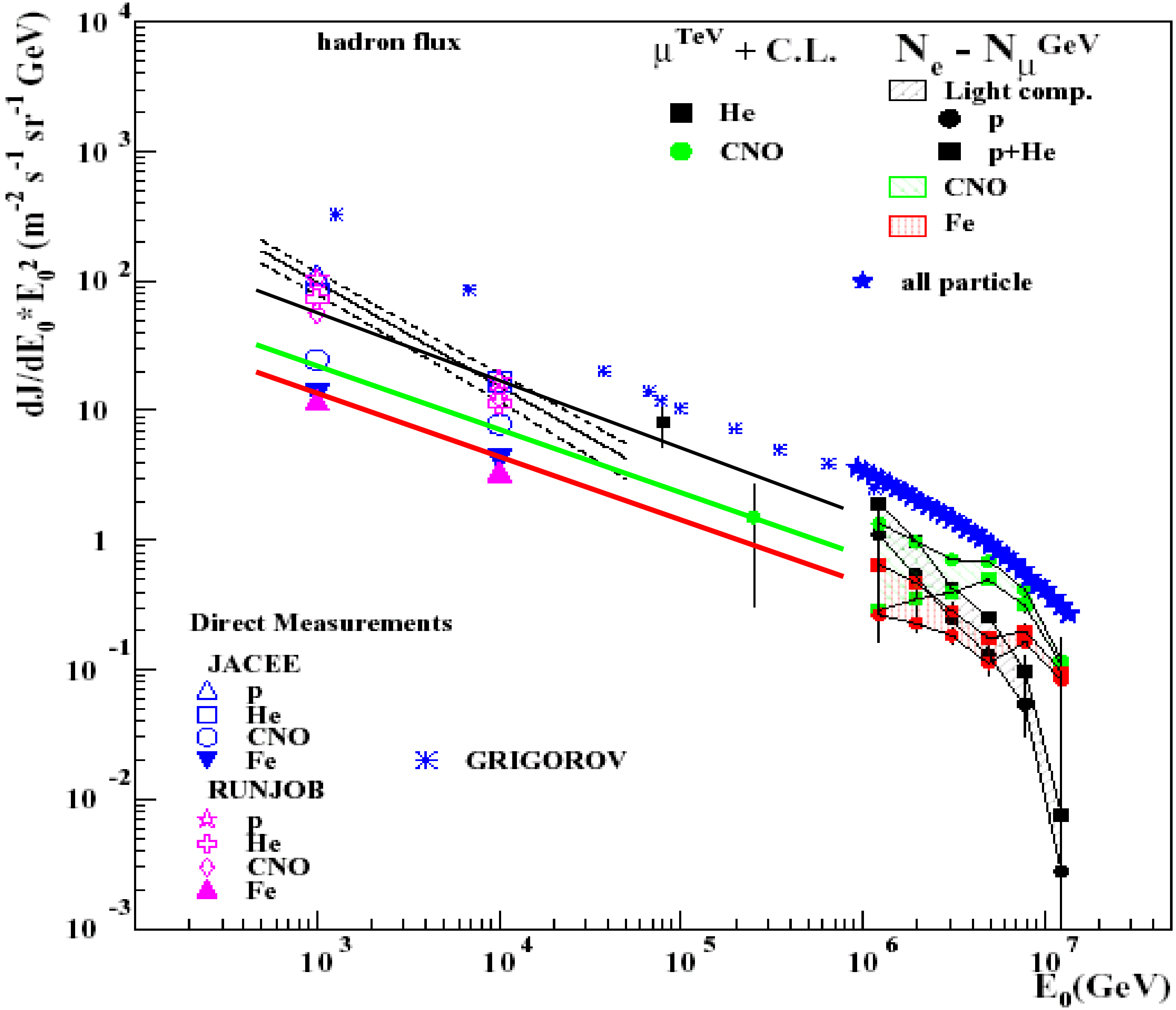

APJ 470 (1996) 501

Cosmic ray anisoptropy at E_0 > 100 TeV

Evolution of the anisotropy in the knee region: test of diffusion model and insight for possible discrimination between:

- energy limit of the acceleration process at the source
- change in the property of CR propagation inside the Galaxy described through diffusion models

Previous results: amplitude and phase well established in the energy interval $10^{11} - 10^{13}$ eV by EAS arrays and underground μ detectors:

- amplitude and phase rather constant over the given energy range:

$$A_{sid} : (3\text{-}6)\ 10^{-4} \quad \Phi : 0 - 4 \text{ h LST}$$

EAS-Top extended the measurements @ 100 TeV showing:

- **$A_{sid} = (3.4 \pm 0.3)\ 10^{-4}$ $\Phi_{sid} = (3.3 \pm 0.4)$ h LST   (10 "σ" level)**
- **Reliability of the observation: Compton-Getting effect in solar time and absence of antisidereal signal**

APJ 692 (2009) L130

Evolution of the cosmic ray anisotropy above 10^{14} eV

Final EAS-Top results @ ≈ 100 and ≈ 400 TeV: 1431 full days (Jan 1992 – Dec 1999)

EAST – WEST method: it removes counting rates differences of atmospheric origin:

- counting rates every 20 min
- Flux inside ± 45° around EAST and WEST directions
- $\theta < 40°$

10^{14} eV: $A_{sid} = (2.6 \pm 0.8)\ 10^{-4}$ $\Phi_{sid} = (0.4 \pm 1.2)$ h LST with Rayleigh imitation probability P = 0.5 %

The result is supported by the observation of the Compton Getty effect due to the revolution of the Earth around the Sun and by the absence of antisidereal effects.

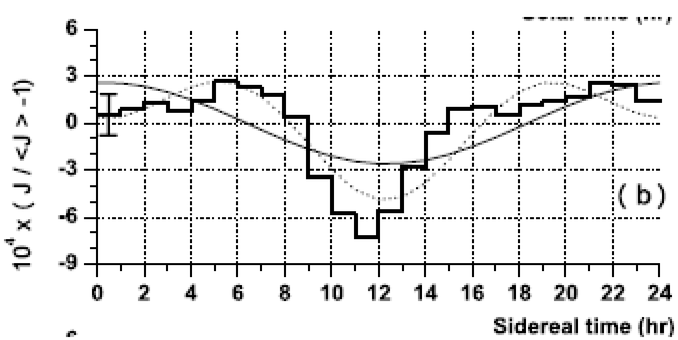

- **Sidereal wave**: shape in remarkable agreement with previous measurements (EAS and underground muon detectors)

APJ 692 (2009) L130

Evolution of the cosmic ray anisotropy above 10^{14} eV

Final EAS-Top results @ ≈ 100 and ≈ 400 TeV: 1431 full days (Jan 1992 – Dec 1999)

EAST – WEST method: it removes counting rates differences of atmospheric origin:

- counting rates every 20 min
- Flux inside ± 45° around EAST and WEST directions
- $\theta < 40°$

4 x 10^{14} eV: the anisoptropy shows a larger amplitude $A_{sid} = (6.4 \pm 2.5)\ 10^{-4}$ and a different phase $\Phi = (13.6 \pm 1.5)$ h LST with an imitation probability P = 3.8 %

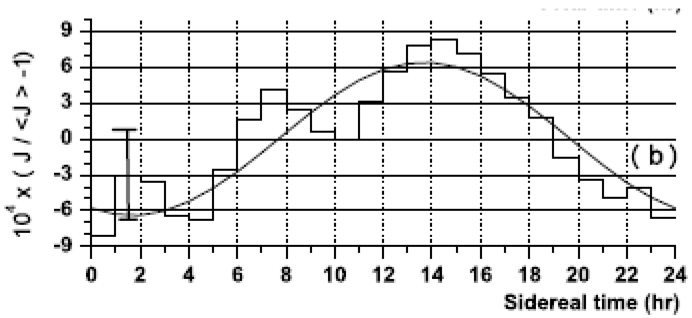

- **Sidereal wave**: rather different from the one at 100 TeV: broad excess around 13-16 h LST, and increased amplitude

Dependence of the anisotropy amplitude over the primary energy (A ∞ Eδ) from the two EAS-Top measurements: $\delta = 0.74 \pm 41$. **Sharp increase aproaching the knee ?**

PRD 79 (2009)

The *p*-air inelastic cross section measurement at √s ≈ 2 TeV

Primary Energy E_0 selected using muon number Nμ

Shower development stage selected using shower size Ne

- The absorption length of cosmic ray proton showers at maximum development in the energy range $E_0 = (1.5 \div 2.5) \cdot 10^{15}$ eV (i.e. at √s ≈ 2 TeV) is measured at the atmospheric depth of 820 g/cm^2

$$\sigma_{p\text{-air}}^{inel} = 338 \pm 21_{stat} \pm 19_{syst} - 29_{syst(He)} \text{ mb}$$

- This value is about 20% smaller than the values in use within most used hadronic interaction models

- Deeper shower penetration in the atmosphere with respect to the predictions of the interaction models

- $\lambda_{obs}^{sim} < \lambda_{obs}^{exp}$

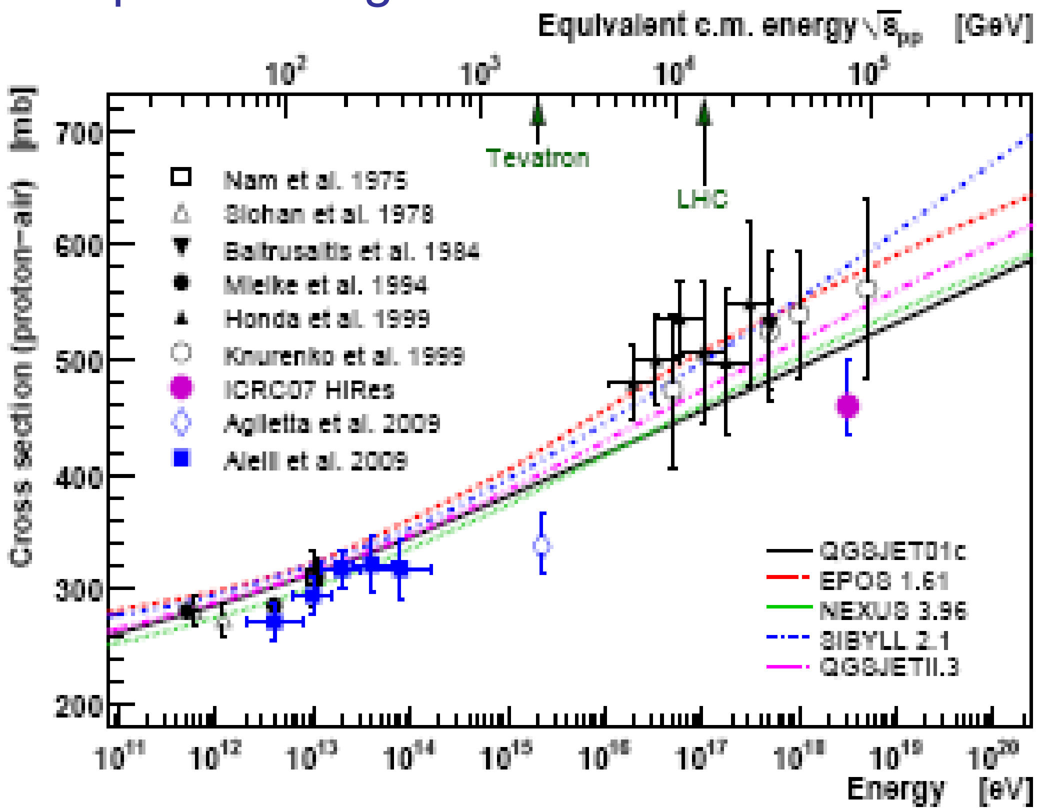

I did not mention:

- Results on candidate UHE γ-ray sources : mainly upper limits on several candidate sources (useful to demonstrate the stability of the array over long periods: i.e. distribution of daily excesses from the source direction)
- Search for γ-ray emission from the galactic disk
- Limit to the rate of ultra high energy γ-rays in the primary cosmic radiation
- Search for γ-ray transients through the Backsan and EAS-Top correlated data
- Search for γ-bursts in coincidence or not with satellites (BATSE)
- Study of horizontal air showers for UHE neutrino detection
- Study of the atmospheric Cherenkov light images from Extensive Air Showers
- Study of the ionizing component during thunderstorms

Conclusion

- The EAS-Top experiment has provided new crucial scientific information on different characteristics (energy spectrum, chemical composition, sidereal anisotropy, gamma ray emission, high energy hadronic interactions) of the high energy cosmic radiation.
- Most of the results are a good reference for the understanding of the c.r. behaviour at higher energies.

Conclusion

- The EAS-Top experiment has provided new crucial scientific information on different characteristics (energy spectrum, chemical composition, sidereal anisotropy, gamma ray emission, high energy hadronic interactions) of the high energy cosmic radiation.
- Most of the results are a good reference for the understanding of the c.r. behaviour at higher energies.

The EAS-Top success is primarily due to its principal investigator: Gianni.


1970
1980
1990
2000
2009
Pic du Midi
A life-long, delicate, subtle, adventuruous
excursion over the CR spectrum
EAS-TOP
Plateau Rosa
Kascade-Grande
Pierre Auger
10¹³ eV
10¹⁴ eV
10¹⁵ eV
10¹⁷ eV
10²⁰ eV

Evolution of composition
$< N_e - N_\mu >$

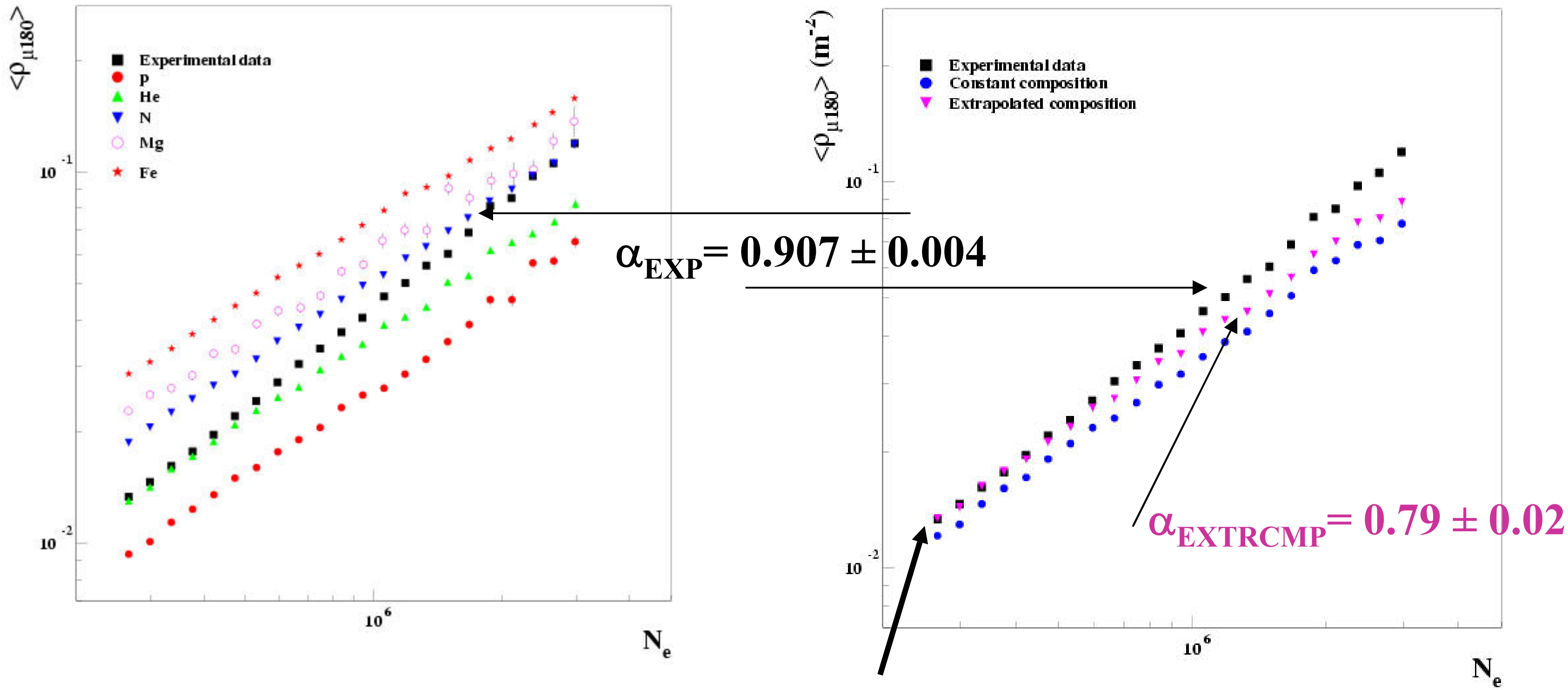

QGSJET: agreement with extrapolated direct measurements!

$\alpha_{MAX\text{-}VENUS} = 0.820 \pm 0.007$

NO INTERACTION MODEL CAN ACCOUNT FOR THE INCREASING N_μ vs. Ne WITHOUT INCREASING PRIMARY MASS

Final EAS-TOP results on large scale CR anisotropy

- confirms amplitude and phase of CR anisotropy **at 10^{14} eV:** $A^I_{sid} = (2.6 \pm 0.8) \cdot 10^{-4}$, $\phi^I_{sid} = (0.4 \pm 1.2)$ **h LST**, with Rayleigh imitation probability $P^I_{sid} = 0.5\%$
- The result is supported by the **observation of the Compton-Getting effect** due to the revolution of the Earth around the Sun, and by the **absence of anti-sidereal effects**
- It confirms the homogeneity of the anisotropy data over the energy range 10^{11}-10^{14} eV
- **At higher energies (around 4×10^{14} eV) the anisotropy shows a larger amplitude, $A^I_{sid} = (6.4 \pm 2.5) \times 10^{-4}$, and a different phase, $\phi^I_{sid} = (13.6 \pm 1.5)$ h LST, with an imitation probability of 3.8% .**

- Dependence of the anisotropy amplitude over primary energy ($A \propto E_0^{\delta}$) from the two EAS-TOP measurements: $\delta = 0.74 \pm 0.41$.
- At least in the energy range $(1-4)\cdot 10^{14}$ eV, dependence compatible with that of the diffusion coefficient as derived by composition measurements at lower energies
- Sharp increase of the anisotropy above 10^{14} eV (i.e. approaching the "knee") indicative of a sharp evolution of the propagation properties, and therefore of the diffusion coefficient ?